Ion Velocity Measurements for the Ionospheric Connections Explorer

R.A. Heelis, R.A. Stoneback, M.D. Perdue, M.P. Depew, Z.A. Morgan, M.D. Mankey, C.R. Lippincott, L.L. Harmon and B.J. Holt.

William B. Hanson Center for Space Sciences
Physics Department, University of Texas at Dallas, Richardson, TX.

Abstract

The Ionospheric Connections Explorer (ICON) payload includes an Ion velocity Meter (IVM) to provide measurements of the ion drift motions, density, temperature and a major ion composition. The IVM will derive these parameters utilizing two sensors, a retarding potential analyzer (RPA) and an ion drift meter (IDM) that have a robust and successful flight heritage. The IVM described here incorporates the most sensitive device that has been fielded to date. It will be used in conjunction with measurements from the other ICON instruments to uncover the important connections between the dynamics of the neutral atmosphere and the ionosphere through the generation of dynamo currents perpendicular to the magnetic field and collisional forces parallel to the magnetic field. Here the configuration and operation of the instrument is described as well as a description of the data that it is expected to return.

1. Introduction

The Ionospheric Connections Explorer (ICON) mission is poised to discover fundamental connections between the dynamics of the neutral atmosphere at altitudes between 100 km and 300 km and the charged particle motion, which is tied to the magnetic field that threads the entire region. A comprehensive description of the links between the charged and neutral species will be revealed with a unique combination of remote measurements of the plasma and neutral density and the neutral winds and in-situ measurements of the plasma density and plasma drift. In-situ determination of the plasma density and plasma drift are made by an Ion Velocity Meter (IVM), a planar detector that measures the energy and the angle of arrival of the thermal ions that move supersonically with respect to the spacecraft. Instruments, utilizing this technique have been successfully deployed on many science missions beginning with OGO6 [Hanson et al. 1970] and continuing through the era of Atmosphere Explorer [Hanson et al., 1973], Dynamics Explorer [Hanson et al, 1981; Heelis et al. 1981], the Defense Meteorological Satellite Program and ROCSAT [Le et al., 2003] and the Coupled Ion Neutral Dynamics Investigation [Heelis et al., 2009].

For the ICON mission this flight-proven approach is further developed and combined with state-of-the-art design in analog and digital electronics to produce a robust and sensitive device that meets the rigorous measurement requirements of the mission. The principles of operation of the IVM sensors have been previously described [Heelis and Hanson1975; 1998] but are reviewed here in the context of the ICON measurement requirements in addition to the specific instrument performance details and the geophysical parameters that will delivered by the instrument.

2. IVM Mechanical Configuration

Figure 1 has three panels showing a photograph of the flight IVM sensor and isometric projections that detail the major mechanical systems. The ICON IVM consists of two planar sensors. A retarding potential analyzer (RPA) and an ion drift meter (IDM) are mounted to view approximately along the spacecraft velocity vector and are optimally configured to accomplish the separate functions of constituent ion energy determination and ion arrival angle respectively. The sensors are attached to a baseplate to which the electronics compartment is affixed at the rear. The rear cover is attached to a flexure mount that provides a mechanical interface to the spacecraft payload interface plate (PIP). The rear cover also contains passive radiator surfaces. In low earth orbit the spacecraft velocity in excess of 7 km s^{-1} provides the constituent ions with mass dependent ram energies $\frac{1}{2} m V_s^2$, of about 0.3 eV/amu and thermal energy widths $m V_s V_{th}$, of about 0.1 eV/amu with respect to the sensor. In order to minimize the effects of the sensors themselves on the plasma, it is important that the local electrostatic environment present small and planar potentials parallel to the instrument aperture plane so that the ion arrival angle and energy distribution are modified in a predictable way by electric fields that are parallel to the sensor look direction. A planar conducting aperture plane, which surrounds the instrument apertures, is utilized to accomplish this task. It is attached to the sensors from the front and also provides key radiative surfaces to dissipate instrument and solar heat inputs. Optimum sensitivity to arrival angle and incident energy is also obtained if the sensor ground reference is maintained near the plasma potential. The spacecraft reference ground with respect to the plasma is dependent on the conducting properties of the spacecraft exposed surfaces and to exposed potentials that may be part of the solar power system. While best practices are employed to maintain a ground reference close to the plasma potential, the IVM sensors are electrically isolated from the spacecraft to provide an independent ground reference that is established by a section of the aperture plane called the "SenPot" surface, which is maintained at the floating potential. Figure 2 shows schematic cross-sections of the RPA and IDM sensors. Each is constructed similarly consisting of a gridded aperture plane and a series of internal planar grids that are precisely positioned using ceramic spacers to maintain parallel potential planes that are biased to provide the appropriate functionality. In both sensors the woven grids are 0.001" diameter gold-plated tungsten wire with a density of 50/inch or 100/inch. The effective area for ion current collection is therefore corrected for the optical transparency of the grid stack.

The RPA presents a gridded circular entrance aperture G1, tied to the sensor ground and a solid collector at which the ion flux is measured as a current. Referring to figure 2, grid G2 is a double retarding grid that is stepped through a series of positive potentials to control the energy of incoming ions that have access to the collector. Grid G3 is negatively biased with respect to the sensor ground to reject thermal electrons incident on the grid and to suppress photoelectrons that are produced from the collector.

The IDM presents a square aperture to the incoming plasma. The grids G3 and G4/G5 are grounded, providing a field-free region through which the supersonic ions flow before forming an image of the aperture on a segmented collector. The grid G6 serves to reject thermal electrons and suppress photoemission from the collector surfaces. The collector is divided into four quadrants with the dividing lines parallel to the aperture edges allowing currents to collector halves to be measured along two mutually perpendicular axes.

The grid G1 forms a grounded plane across the aperture while a repeller grid G2 precedes the square entrance aperture of the IDM. This grid serves to reject the admission of H+ ions that may have thermal speeds that are comparable to the spacecraft velocity. In such a circumstance, thermal spreading of the beam beyond the instrument aperture produces a sensitivity to angle that is different from that of the heavier ions. The removal of this signal allows the arrival angle associated with the bulk flow of all the species to be determined from the signal dominated by the heavy supersonic O+ ions.

3. Principles of Operation

3.1 Retarding Potential Analyzer (RPA)

The RPA views approximately along the spacecraft velocity vector and has a small entrance aperture compared to the collector size. Within the instrument a retarding grid is stepped through a sequence of potentials, which determine the energy of the incoming ions that have access to the collector. The expected range in the angle of arrival of the ions is small (<5°) compared to the angular acceptance of the instrument and thus the current collected may be simply obtained by integrating the one-dimensional flowing Maxwellian distribution function along the instrument look direction from infinity to the velocity of the ions that will be stopped by the potential on the grid as seen by the plasma. The current for a single ion species of mass *m* and number density N_i is given by

$$I(\phi) = qA_{eff}\frac{N_i}{2}V_r\left[1 + erf(\beta f) + \frac{1}{\sqrt{\pi}\beta V_r}\exp\left(-\beta^2 f^2\right)\right]$$

where A_{eff} is the effective area of the collector, $f = V_r - (2q\phi/m)^{1/2}$, with *q* the electron charge, represents the average velocity of the ions that have access to the collector and $\beta = (m/2kT_i)^{1/2}$, is the reciprocal of the thermal velocity of the ions. Here, $V_r = (\vec{V}_d + \vec{V}_s)\cdot\hat{n}$ is the total velocity of the ions given by the sum of the ambient ion drift $\vec{V}_d$ and the spacecraft velocity $\vec{V}_s$ and $\hat{n}$ is the unit vector along the sensor look direction. $\phi = R_v + \psi_s$, is the potential on the grid as seen by the plasma and is thus the sum of the retarding potential R_v with respect to the sensor ground and the sensor ground potential with respect to the plasma ψ_s. The measured current will be the sum of currents for all constituent ions that are present. The current at zero retarding potential provides the total plasma number density and a least squares fitting procedure, applied to the normalized current-voltage characteristic, yields a common temperature, a bulk flow velocity for the ions and the fractional population of the major constituent ions. In addition, the sensor plane potential with respect to the plasma is also retrieved. Corrections to account for the lack of perfect potential planes produced by wire grids are also included in the fitting procedure [Stoneback et al., 2016].

Figure 3 shows typical current voltage characteristics obtained from the RPA aboard the Communication Navigation Outage Forecast System (C/NOFS) satellite. In each panel the open symbols denote the retrieved data and the solid line represents the result of the fitting procedure with the results shown to the right of the current-voltage characteristic in each panel. In panel A is data taken near 650 km altitude and 05:25 local time indicating the presence of a small fractional population of H+ in addition to the major ion, O+. Note that the I-V characteristic represents the integral contribution from all species that are present and the major species are distinguished by the differences in their ram energy as mentioned previously. A simple examination of the relative values of the ion current near zero volts and 3 volts can therefor detect the presence of light ion species and thus indicate the masses that need to be considered in the least squares analysis procedure.

In panel B is shown the I-V characteristic taken near 500 km altitude and 14:30 local time where O+ is the only ion present.

3.2 Ion Drift Meter (IDM)

The IDM also views approximately along the spacecraft velocity vector and uses a simple geometric relationship between the arrival angle of the incoming ion beam and the area illuminated, and thus the current collected, at the collector segments. Figure 4 shows a schematic representation of the ion beam (in red) and its displacement along one axis aligned with an aperture edge within the field-free region of the sensor. The collector quadrant dividing lines and aperture edges are aligned with the local horizontal and the local vertical so that by appropriately configuring collector halves, the arrival angle in each of these planes containing the unit vectors $\hat{h}$ and $\hat{z}$ respectively, can be measured. The ratio of the collector currents, which are each proportional to the area illuminated, are given in terms of the sensor dimensions and the arrival angle by $\frac{I1}{I2} = \frac{W/2 + D\tan\alpha}{W/2 - D\tan\alpha}$. Thus by measuring the current ratio we may determine the ion arrival angle. The corresponding transverse drift velocity is given by $\left(\vec{V}_d + \vec{V}_s\right)\cdot\hat{t} = \left[V_r^2 - {2q\psi_s}/{m}\right]^{1/2}\tan\alpha$ where $\hat{t}$ is the unit vector along the selected transverse direction. Close inspection of figure 4 shows that the arrival angle must be corrected for the displacement of the beam produced by the suppressor grid. In addition, the suppression of photoemission from the collector can lead to some current exchange between the collector halves and correction procedures to account for this effect are also applied [Stoneback et al, 2014]

4. IVM Electrical Configuration

Figure 5 shows a block diagram of the major electrical subsystems that make up the IVM. In the RPA, the retarding potential is generated through the contents of a memory block containing 32 discrete levels that are used to generate a voltage that is known to an accuracy of 0.001V. At each step the dwell time is approximately 32 milliseconds allowing the content of the memory block to be executed in one second. The content of the memory that describes the sweep format is designed to optimize the point distribution based on the environment that the satellite encounters. While experience allows a well-informed distribution of points to define a default sweep, the content of the sweep memory made be changed by command from the ground. The potential on the suppressor grid, to reject thermal electrons and suppress photoemission currents from the collector, may also be changed between 0V and -10.5V by ground command. It will be adjusted to provide the minimum required voltage to accomplish these two tasks. An automatically ranging linear electrometer measures the ion current after the retarding grid is stepped to a discrete potential. The electrometer has 8 sensitivity ranges, decreasing by approximately the square-root of ten, allowing currents between 50pA and 3.9mA to be measured. At each step the RPA output consists of the memory location that provides the retarding voltage, the current recorded with 14-bit accuracy and accompanied by 3 bits that designate the electrometer sensitivity level.

The IDM has two grid potentials that may be changed by ground command. As in the RPA the rejection of thermal electrons and the suppression of photoemission is accomplished with a suppressor grid, which precedes the collector and may be changed between 0V and -10.5V. In addition a repeller grid may be biased with a potential between 0V and 3.5V V to reject the admission of H+ ions that have thermal speeds comparable to the spacecraft velocity.

Switches at the collector allow the segments to be combined to provide a current from collector halves that are aligned either along the local horizontal or the local vertical axis. For a designated axis the current from each collector half is measured by a logarithmic electrometer having a dynamic range from 250 pA to 9.5 µA, which is subsequently registered with 14-bit accuracy for transmission to the ground. The outputs from each logarithmic electrometer are sampled at 16 Hz. The output for each logarithmic electrometer also provides the input to a linear difference amplifier that delivers the ratio of the ion currents to be used in the expression described earlier to derive the ion arrival angle. The output of the difference amplifier is recorded with 14-bit accuracy and accompanied by 1 bit (axis) that describes the collector halves orientation (horizontal or vertical) and 1 bit (polarity) designating which collector half is collected to which logarithmic electrometer. The difference amplifier outputs and configuration indicators are sampled at 32 Hz. The instrument may be configured by ground command to alternate between horizontal and vertical arrival angles with a 16 Hz or 8 Hz cadence or to remain measuring a fixed axis arrival angle (horizontal or vertical). In both cases biases in the logarithmic electrometers are removed by periodically changing the polarity of the inputs.

The reference ground for both sensors is driven away from the spacecraft ground to reside at the same potential as the floating reference surface called SenPot. The instrument signals are optically coupled to the spacecraft command and data system to accommodate the difference between the spacecraft and sensor ground potentials.

5. Instrument Calibration

The RPA utilizes an automatic ranging linear amplifier for which the voltage output is given by $V = G_i I + O_i$ where G_i is the sensitivity at level i and O_i is the electrometer offset associated with sensitivity level *i.* The sensitivity and offset for each level is established in the laboratory using a calibrated and certified current source that is directly applied to the collector. By injecting current over the full range, the output at all sensitivity levels can be obtained and linear straight-line fitting is utilized to establish the sensitivity and offset for each level. This procedure is repeated over the range of operating temperatures expected for the instrument. A calibration mode that fixes the retarding potential and steps through the different sensitivity levels may be exercised in flight to verify and update the laboratory calibration files if appropriate. The retarding voltage is generated utilizing a d/a converter and the voltage for each digital level is recorded over the expected operating temperature range in the laboratory with xx mV accuracy. The electrometer calibration and retarding voltage calibration data are retained for use in the data reduction procedure exercised on the ground.

The IDM utilizes a linear difference amplifier to determine the ratio of input currents that are measured using logarithmic electrometers. The logarithmic electrometers are designed with the same sensitivity level, but may have different offsets. Thus the voltage proportional to the current ratio, from which the ion arrival angle is determined is given by

$$V = G_d\left[G\log {}^{I_1}\!/\!{}_{I_2} + O_a - O_b\right] + O_d = G_s\log {}^{I_1}\!/\!{}_{I_2} + O_l + O_d .$$

The overall system sensitivity level, G_s is determined in the laboratory by utilizing a calibrated and certified current source to inject a known current ratio directly to the sensor collectors. The offset, which has contributions from both the difference amplifier and the logarithmic electrometers, may be reduced to that originating from the difference amplifier alone by repeating the calibration procedure with the inputs to the logarithmic electrometers inverted. Then the voltage proportional to the current ratio, from which the ion arrival angle is determined, is given by $V = G_d\left[G\log {I_1}/{I_2} + O_b - O_a\right] + O_d = G_s \log {I_1}/{I_2} - O_l + O_d$. The two calibration curves may then be added to remove the offset from the logarithmic electrometers. The sensitivity level and offset is again retained for use in the ground data processing. In flight verification and adjustment of the calibration data may be obtained from maneuvers for which the reference axes of the spacecraft are known precisely. These may be undertaken for calibration of the optical instruments and for changes in the observational configuration of the payload.

6. IVM Specifications and Performance

Table 1 details the instrument physical properties. The modest power requirements allow the sensor to be operated with a 100% duty cycle. However operation of the IVM on ICON will be performed by two identical configurations of the sensors allowing an interchange between ram and wake that is required for the optical instruments to view on either side of the satellite orbit plane. The IVM, either the IVM-A or IVM-B instrument, will be operated continuously when it is pointed nominally in the ram direction and will continue to operate during slewing maneuvers to re-orient the satellite for calibrations of the optical instruments [refs]. During continuous operations, the RPA is configured to produce current-voltage characteristics at 1 Hz rate. The IDM will nominally alternate between measurement of the horizontal and vertical ion arrival angles so that each are obtained at 8 Hz. This operational mode of the instrument is expected to dominate the data obtained throughout the mission. However, changes in the operational profile are possible to allow acquisition of current-voltage curves at 2Hz and 32Hz sampling of a fixed ion arrival angle. Data from the IVM are packaged for a 4-second period and the content of a data packet is independent of the mode of instrument operation and configuration of the other grid potentials. This additional information is included in the header of each 4-second data packet allowing autonomous processing of the data in each packet.

7. Instrument Operations and Geophysical Parameters

The principles of operation of the RPA described above show that the total ion number density, the major ion fractional composition, the ion temperature and the ion drift speed along the sensor look direction, are derived in a straightforward way. The analysis procedure also yields a value for the sensor plane potential with respect to the plasma, which is expected to be a weak function of the electron temperature and can be used to continuously assess the quality of the least squares fitting process. The drift speed along the sensor look direction and the sensor plane potential are used in turn to derive the transverse (horizontal and vertical) components of the ion drift vector in the sensor reference frame. It should be emphasized that the derived ion drift vector comprises the sum of the ambient plasma drift, with which we conduct science investigations and the spacecraft velocity vector. The spacecraft velocity vector is specified in a spacecraft reference frame and the sensor look directions are also specified in this reference frame by an alignment procedure conducted on the ground prior to launch. The spacecraft attitude determination system provides the spacecraft velocity in the spacecraft reference frame and it is thus a straightforward exercise to remove the spacecraft velocity to specify the ambient ion drift vector in the sensor reference frame.

More useful to the scientist and to the removal of systematic offsets in the data, is an expression of the plasma drift in magnetic coordinates that specify the plasma drift parallel and perpendicular to the local magnetic field. The unit vectors that define the directions along the magnetic field and perpendicular to the magnetic field in the meridian and perpendicular to the meridian, are determined from the inertial attitude of the spacecraft and the International Geomagnetic Reference Field (IGRF) [Finlay et al., 2010].

Once expressed in magnetic coordinates two different conditions may are applied to remove systematic dc offsets that may exist due to errors in the specification of the instrument pointing with respect to the spacecraft reference axes. First, it may be recognized that averages of the vertical (meridional) plasma drift in longitude and local time must be zero in order to satisfy the requirement that the field be electrostatic and that $\nabla \times \vec{E} = 0$. Second, the plasma density in the middle ionosphere is sufficiently high and the ion-neutral collision frequency sufficiently low that magnetic flux lines may be regarded as electric equipotentials. Thus a condition for conjugacy in the magnetic east-west drift is imposed on the average measurements taken in restricted local time and longitude sectors. These two conditions allow the removal of offsets in the transverse drifts computed by the IDM in a manner described in more detail by Stoneback et al. [2012]. Table 2 lists the parameters that will be retrieved during the operation of the IVM.

The IVM derived parameters of primary interest to the ICON science objectives are also those derived from the IVM that was part of the payload for the Coupled Ion Neutral Dynamics Investigation (CINDI). Figure 6 shows an example of one day of these key parameters as illustrative of the information that will be provided by the IVM for ICON. In this display the primary variations around the orbit are produced by local time and altitude, while for the ICON orbit the variations will be dominated by local time and latitude. Each orbit traverses the equatorial region at a different longitude and thus the variations seen here during one day reflect variations in longitude as will also be the case for ICON. Key to the science objectives of the ICON mission are comparisons of the longitude variations in the zonal and meridional drifts with the corresponding wind fields observed by MIGHTI and weighted by the ionospheric conductivity determined by the neutral and ion density profiles derived by FUV and EUV.

8. Summary

The ICON mission brings together for the first time a unique set of measurements of the neutral and charged particle number density and drift motions to enable the connections between the dynamo action of the winds and the drift motions of the plasma to be revealed. The IVM instrument, which provides the measurements of plasma drift, is based on a strong heritage from previous missions and incorporates the most capable electrical and mechanical designs, while capitalizing on previous experience in data retrieval and reduction procedures. The resulting measurements are expected to uncover systematic longitude variations in the plasma drift associated with tidal modes in the neutral atmosphere as well determine the importance of altitude variations in the wind on the electrodynamics of the F region plasma.

References

Finlay et al., (2010), International Geomagnetic Reference Field: the eleventh generation, Geophys. J. Int. 183 (3): 1216-1230, doi: 10.1111/j.1365-246X.2010.04804.x

Hanson, W. B., S. Sanatani, D. Zuccaro, and T. W. Flowerday (1970), Plasma measurements with the retarding potential analyzer on Ogo 6, J. Geophys. Res., 75(28), 5483–5501, doi:10.1029/JA075i028p05483.

Hanson, W. B., D. R. Zuccaro, C. R. Lippincott, and S. Sanatani (1973), The retarding-potential analyzer on Atmosphere Explorer, Radio Sci., 8(4), 333–339, doi:10.1029/RS008i004p00333.

Hanson, W.B., R.A. Heelis, R.A. Power, C.R. Lippincott, D.R. Zucarro, L.H. Harmon, B.J. Holt, J.E. Doherty and R.A. Power (1981), The ion drift meter on Dynamics Explorer-B. Space. Sci. Instrum., 5, 503-510.

Heelis, R.A., W.B. Hanson, W.B., C.R. Lippincott, D.R. Zucarro, B.J. Holt, L.H. Harmon and S. Sanatani (1981), The retarding potential analyzer on Dynamics Explorer-B. Space. Sci. Instrum., 5, 503-510.

Heelis, R.A., and W.B. Hanson (1975), Techniques for measuring bulk gas motions from satellites, Space Sci. Instrum., 1,493-524.

Heelis, R.A., and W.B. Hanson (1998), Measurements of thermal ion drift velocity and temperature using planar sensors. American Geophysical Union Monograph, Measurement Techniques in Space Plasmas: Particles, doi: 10.1029/GM102p0061.

Heelis, R. A., W. R. Coley, A. G. Burrell, M. R. Hairston, G. D. Earle, M. D. Perdue, R. A. Power, L. L. Harmon, B. J. Holt, and C. R. Lippincott (2009), Behavior of the O+/H+ transition height during the extreme solar minimum of 2008, Geophys. Res. Lett., 36, L00C03, doi:10.1029/2009GL038652.

Le, G., C.-S. Huang, R. F. Pfaff, S.-Y. Su, H.-C. Yeh, R. A. Heelis, F. J. Rich, and M. Hairston (2003), Plasma density enhancements associated with equatorial spread *F*: ROCSAT-1 and DMSP observations, J. Geophys. Res., 108, 1318, doi:10.1029/2002JA009592, A8.

Acknowledgements

This work is supported by NASA grant NNG12FA44C. Successful conduct of the ICON mission and the IVM instrument is the result of key collaborations between teams at the University of California Berkeley, the University of Texas at Dallas and Orbital ATK. We thank the many participants from all these institutions that have resulted in this contribution to the ICON mission.

Mass	4.25 Kg
Power	2.5 W
Volume : Sensor Package	11” x 6.2”x 4.8”
Aperture Plane	15.3” x 11”
Telemetry	2048 bps
Pointing	5°
Pointing Knowledge	0.03°
Instantaneous Field of View	45°

Table 1. ICON IVM Instrument Resources.

Parameter	Range	Accuracy
Cross Track Ion Drift	-750 to 750 ms^{-1}	±3 ms^{-1}
Ram Ion Drift	-500 to 500 ms^{-1}	±12 ms^{-1}
Total Ion Number Density	1.5×10^3 to 5×10^6 cm^{-3}	$\pm 1 \times 10^3$
Major Ion Constituents	0-100%	±2%
Ion Temperature	400 to 10000 °K	±100 °K
Sensor Plane Potential wrt Plasma	-3 to +2 V	±0.01V

Table 2. ICON IVM Measured Parameters

Figure Captions

Figure 1. Photographs of ICON IVM mounted to dummy PIP interface.

Figure 2. Schematic cross sections showing grid configurations for the Retarding Potential Analyzer and the Ion Drift Meter.

Figure 3. Representative current voltage characteristics obtained from the RPA on CINDI. ICON IVM will operate similarly.

Figure 4. Schematic cross-section showing ion beam trajectory through the ion drift meter

Figure 5. Simplified electrical block diagram indicating major subsystems in the ICON IVM.

Figure 6. Representative geophysical parameters derived from the IVM. Shown here is a typical day od measurements taken from the IVM on C/NOFS.

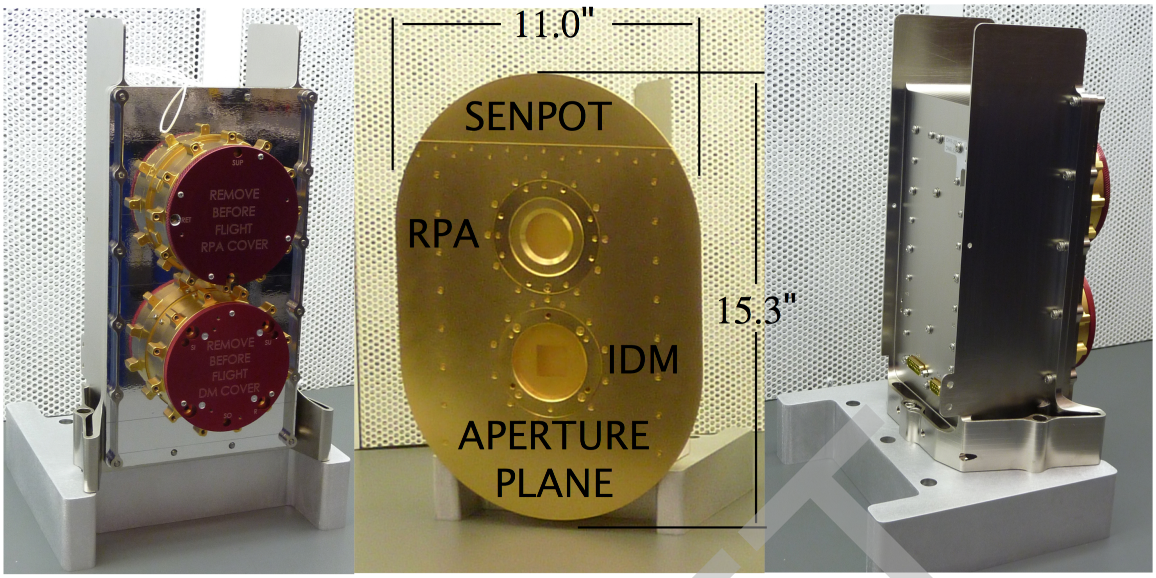
REMOVE
BEFORE
FLIGHT
RPA COVER
REMOVE
BEFORE
FLIGHT
DM COVER
11.0"
SENPOT
RPA
15.3"
IDM
APERTURE
PLANE

FIGURE 1

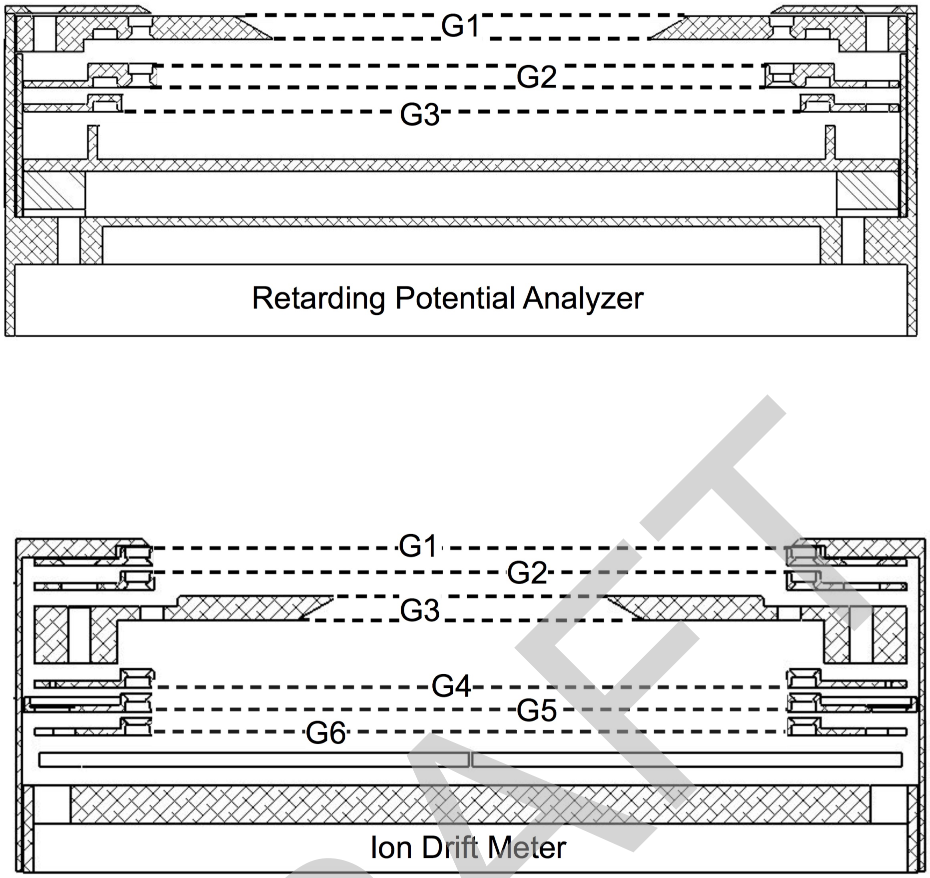
G1
G2
G3
Retarding Potential Analyzer
G1
G2
G3
G4
G5
G6
Ion Drift Meter

FIGURE 2.

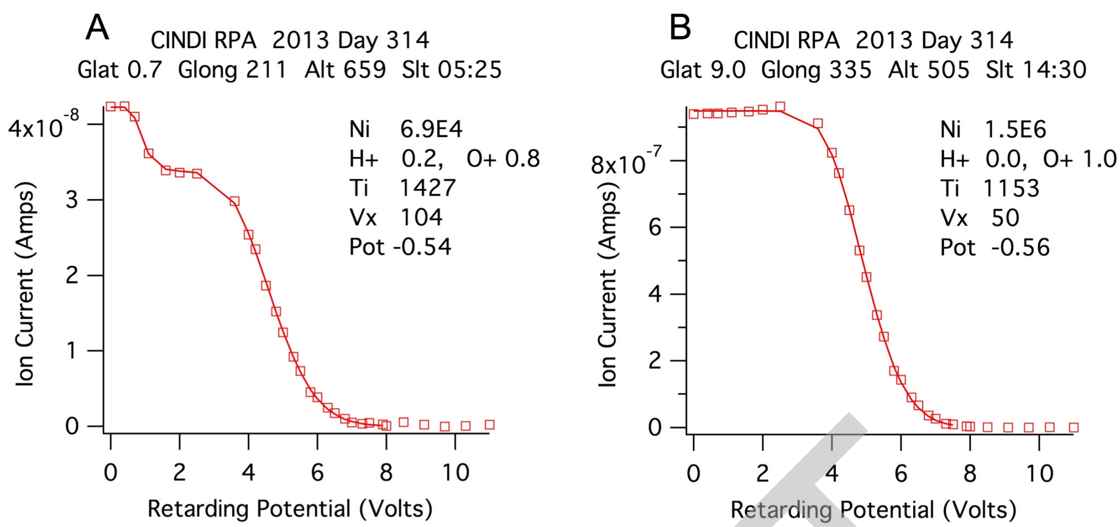
A
CINDI RPA 2013 Day 314
Glat 0.7 Glong 211 Alt 659 Slt 05:25
Ni 6.9E4
H+ 0.2, O+ 0.8
Ti 1427
Vx 104
Pot -0.54
Ion Current (Amps)
Retarding Potential (Volts)
B
CINDI RPA 2013 Day 314
Glat 9.0 Glong 335 Alt 505 Slt 14:30
Ni 1.5E6
H+ 0.0, O+ 1.0
Ti 1153
Vx 50
Pot -0.56
Ion Current (Amps)
Retarding Potential (Volts)

FIGURE 3

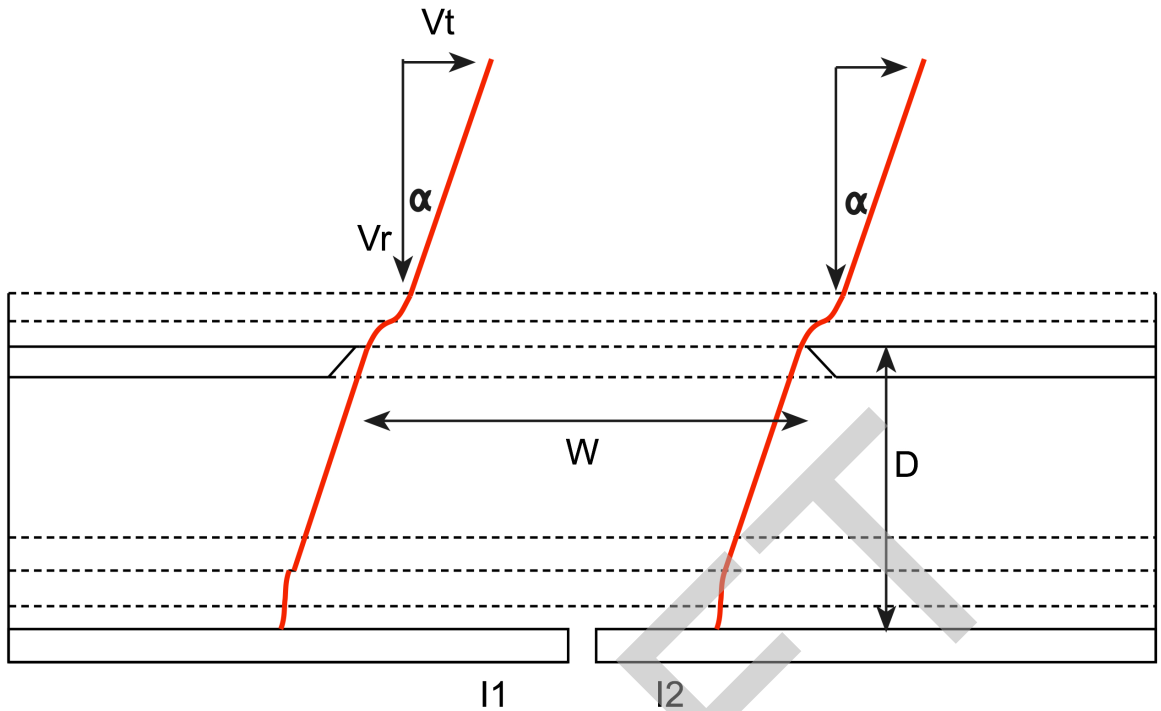

FIGURE 4

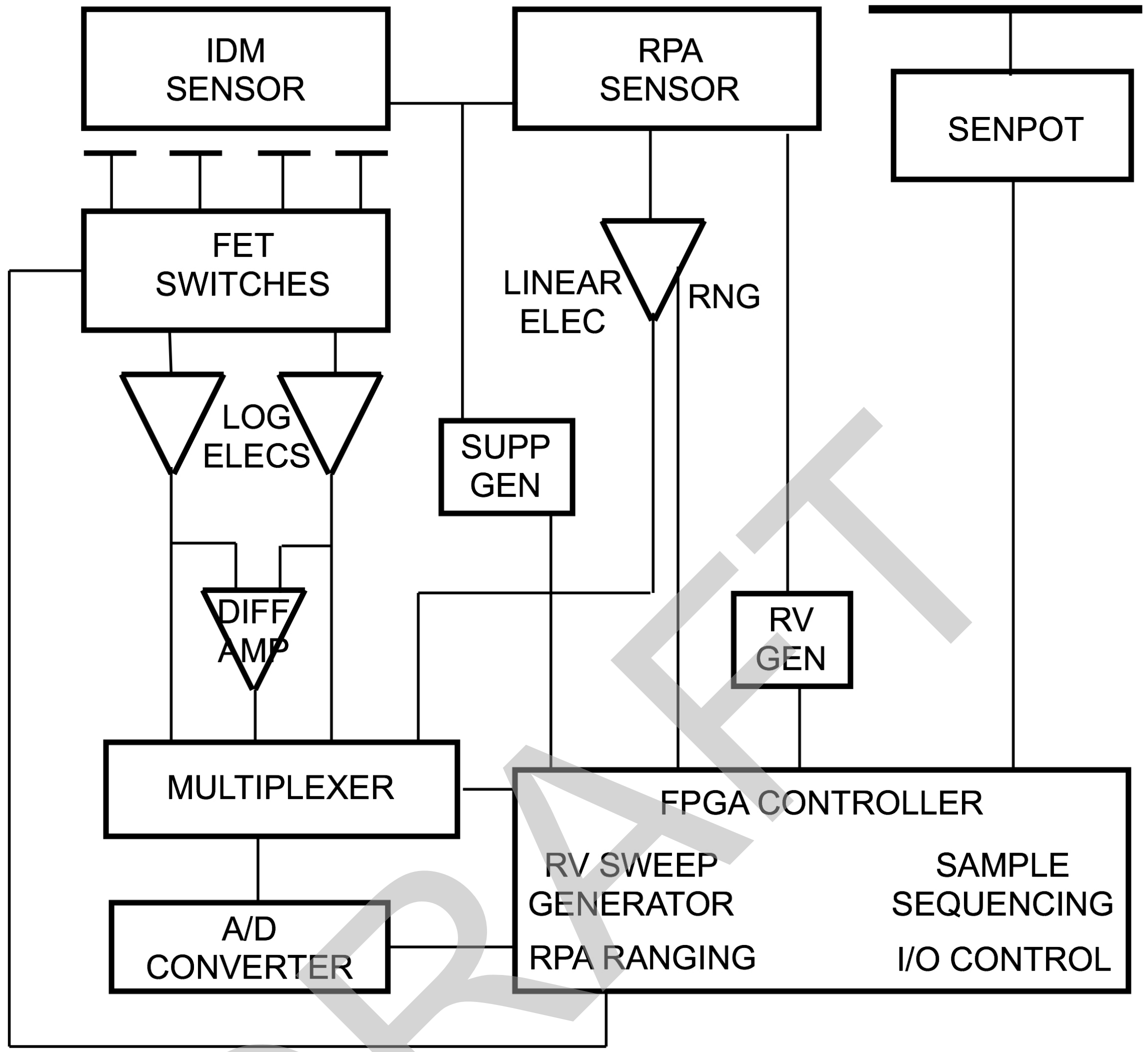
IDM
SENSOR
RPA
SENSOR
SENPOT
FET
SWITCHES
LINEAR
ELEC
RNG
LOG
ELECS
SUPP
GEN
DIFF
AMP
RV
GEN
MULTIPLEXER
FPGA CONTROLLER
RV SWEEP
GENERATOR
SAMPLE
SEQUENCING
RPA RANGING
I/O CONTROL
A/D
CONVERTER

FIGURE 5

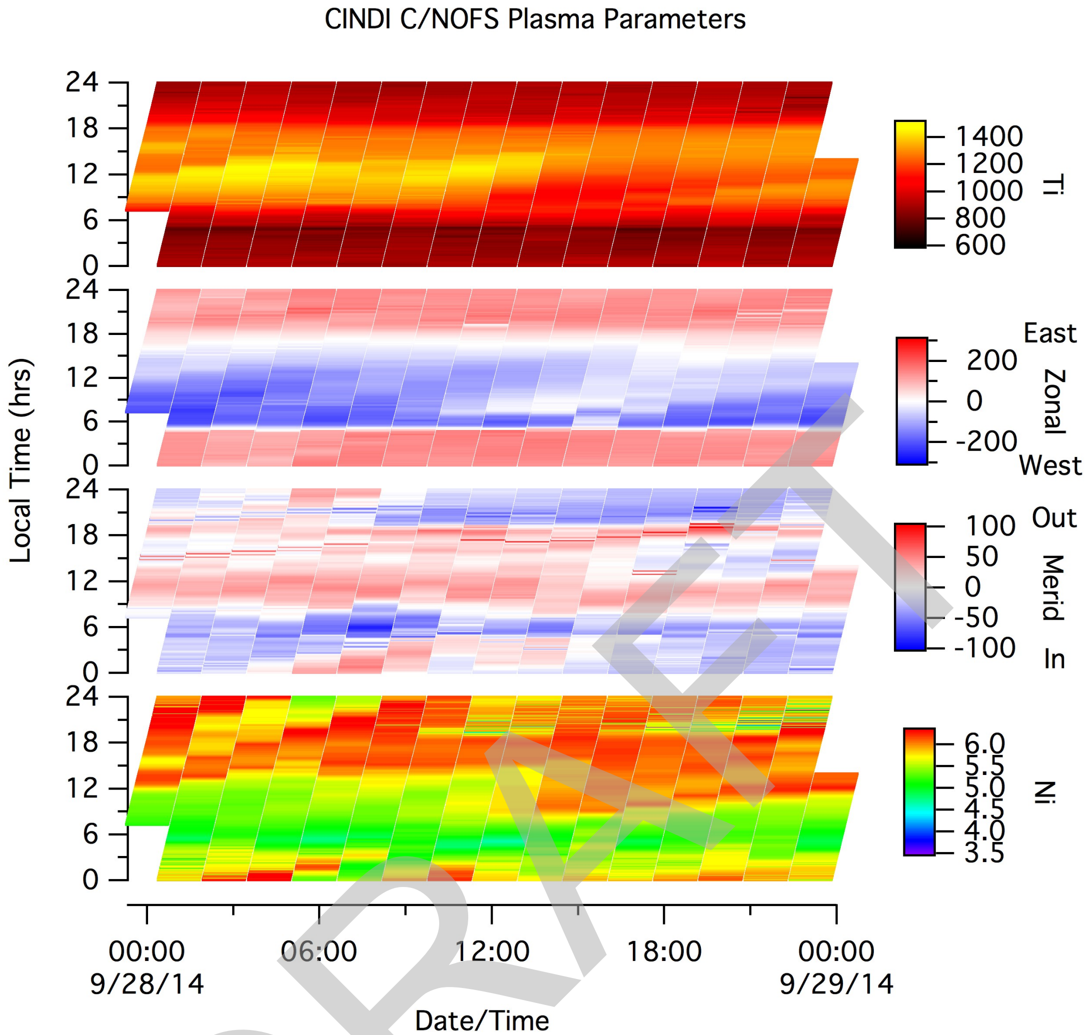

CINDI C/NOFS Plasma Parameters
Local Time (hrs)
24
18
12
6
0
1400
1200
1000
800
600
Ti
East
200
0
-200
West
Zonal
100
50
0
-50
-100
Out
Merid
In
6.0
5.5
5.0
4.5
4.0
3.5
Ni
00:00
9/28/14
06:00
12:00
18:00
00:00
9/29/14
Date/Time

FIGURES 6